

Red-Light-Controllable Liquid-Crystal Soft Actuators via Low-Power Excited Upconversion Based on Triplet–Triplet Annihilation

Zhen Jiang,^{†,§} Ming Xu,^{‡,§} Fuyou Li,^{*,‡} and Yanlei Yu^{*,†}

[†]Department of Materials Science & State Key Laboratory of Molecular Engineering of Polymers, Fudan University, Shanghai 200433, China

[‡]Department of Chemistry & Institutes of Biomedical Sciences, Fudan University, Shanghai 200433, China

S Supporting Information

ABSTRACT: A red-light-controllable soft actuator has been achieved, driven by low-power excited triplet–triplet annihilation-based upconversion luminescence (TTA-UCL). First, a red-to-blue TTA-based upconversion system with a high absolute quantum yield of $9.3 \pm 0.5\%$ was prepared by utilizing platinum(II) tetraphenyltetrabenzoporphyrin (PtTPBP) as the sensitizer and 9,10-bis(diphenylphosphoryl)anthracene (BDPPA) as the annihilator. In order to be employed as a highly effective phototrigger of photodeformable cross-linked liquid-crystal polymers (CLCPs), the PtTPBP&BDPPA system was incorporated into a rubbery polyurethane film and then assembled with an azotolane-containing CLCP film. The generating assembly film bent toward the light source when irradiated with a 635 nm laser at low power density of 200 mW cm^{-2} because the TTA-UCL was effectively utilized by the azotolane moieties in the CLCP film, inducing their *trans*–*cis* photoisomerization and an alignment change of the mesogens via an emission–reabsorption process. It is the first example of a soft actuator in which the TTA-UCL is trapped and utilized to create photomechanical effect. Such advantages of using this novel red-light-controllable soft actuator in potential biological applications have also been demonstrated as negligible thermal effect and its excellent penetration ability into tissues. This work not only provides a novel photomanipulated soft actuation material system based on the TTA-UCL technology but also introduces a new technological application of the TTA-based upconversion system in photonic devices.



INTRODUCTION

Light-driven soft actuators have a unique capacity to directly convert light energy into mechanical work and act by remote, instant, and precise control.¹ Among these materials, cross-linked liquid-crystal polymers (CLCPs) containing photochromic moieties such as azobenzene may represent one of the most studied systems.^{2,3} Upon irradiation of UV light, *trans*–*cis* photoisomerization of the azobenzene moieties in the CLCPs is triggered, which leads to the change on the alignment of the mesogens; subsequently, the significant macroscopic photodeformation of the whole materials in the form of contraction⁴ and bending^{5,6} was induced due to the cooperative motion of mesogens and polymer segments. Furthermore, these photodeformable CLCPs have been developed as various soft actuators such as plastic motors,⁷ inchworm-like walkers,⁸ flexible microrobots,^{6a} high-frequency oscillators,⁹ and artificial cilia.¹⁰

However, most of the reported photodeformable CLCP systems were manipulated by ultraviolet (UV) or short-wavelength visible light. Such high-energy light is not ideal for practical applications, due to considerations of safety, power consumption, and cost. In order to make CLCPs responsive to longer-wavelength light, several groups had incorporated carbon nanotubes (CNTs) or infrared (IR)-absorbing dyes

into thermoresponsive CLCPs to obtain near-infrared (NIR) or IR-light-induced deformation.¹¹ In this case, the CNTs or IR-absorbing dyes served as a nanoscale heat source to absorb and transform NIR or IR light energy into thermal energy, which subsequently induce the LC isotropic thermal phase transition and thus the contraction or bending of the thermoresponsive CLCPs.

As for the azobenzene-containing CLCPs, introducing the upconversion materials which are capable of conversion of a low-energy photon into a high-energy one^{12–14} could represent another effective and creative way to develop longer-wavelength light-controllable CLCPs. For example, most recently, we have incorporated lanthanide upconversion nanophosphors NaY-F₄:Yb,Tm (~70 nm) into the azotolane-containing CLCP film and succeeded in generating bending of the resulting composite film upon exposure to continuous-wave (CW) NIR light at 980 nm.¹⁵ However, a high excitation power density of 15 W cm^{-2} and resulting overheating effect limit their potential applications. Therefore, it is required to develop new upconversion materials with low-power excitation as well as little excitation light-induced thermal effect.

Received: June 19, 2013

Published: October 2, 2013

A dual-dye upconversion system based on triplet–triplet annihilation (TTA) is a potential candidate as low-power excited, long-wavelength phototrigger of the azotolane CLCPs. This TTA-based upconversion luminescence (TTA-UCL) process shows several advantages over the lanthanide upconversion techniques, such as higher quantum efficiency, larger absorption efficiency, and low excitation power density.^{13,16–22} To date, the reported highly effective TTA-UCL emissive systems, such as green-to-blue emissive PdOEP&DPA^{17c,d,f,g,21a} and red-to-green/yellow emissive PtTPBP&BODIPY (see Supporting Information, Scheme S1),^{17a,18b} exhibit relatively small anti-Stokes shift of ~100 nm. Therefore, when used as the phototrigger of the azotolane CLCP, the green/yellow UCL emission of PtTPBP&BODIPY cannot match the strong absorption band between 400 and 500 nm of the azotolane-containing CLCP well^{6a,c} and the excitation of PdOEP&DPA is green light, whose wavelength is not long enough to avoid the direct absorption by the azotolane CLCP.

To achieve effective UCL-triggered photodeformable CLCP materials, it is necessary to obtain a UCL emissive system with a low-energy excitation light source (such as red laser, $\lambda_{\text{ex}} = 635$ nm), large anti-Stokes shift of >150 nm, and high UCL efficiency. In the present study, we demonstrated a fluorescent dye 9,10-bis(diphenylphosphoryl)anthracene (BDPPA) as the annihilator to fabricate a highly effective red-to-blue TTA-based upconversion system with Pt(II) complex tetraphenyltetra-benzoporphyrin (PtTPBP) as the sensitizer (Scheme 1a). Upon

such as negligible thermal effect and excellent penetration ability of 635 nm light through biological samples.

EXPERIMENTAL SECTION

Materials. All reagents and solvents were used as received without further purification unless otherwise indicated. PtTPBP was purchased from Luminescence Technology Corp. Analytical grade toluene, methanol, CHCl_3 , CH_2Cl_2 , tetrahydrofuran (THF), and dimethylformamide (DMF) were purchased from Sinopharm Chemical Reagent Co., Ltd. Deionized water was used in the experiments throughout. BDPPA was synthesized according to the previous literature (see Supporting Information).²³ The LC compounds **1** and **2** were prepared according to our published work.⁶ Polyurethane was purchased from Aldrich. The thermal initiator (2,2'-azobis(*N*-cyclohexyl-2-methylpropionamide) was purchased from Wako Pure Chemical.

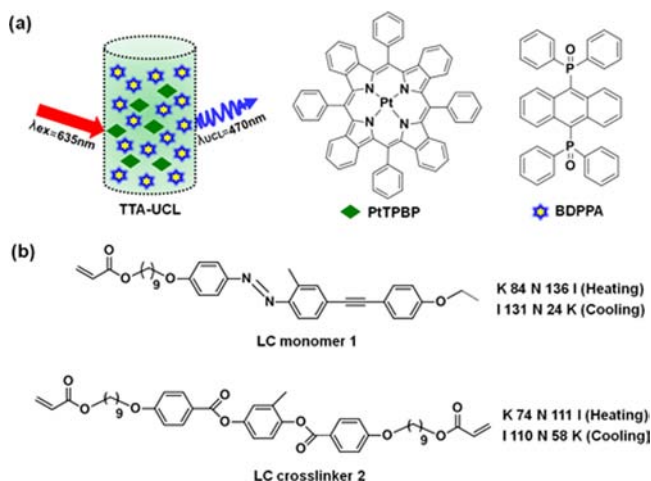
Preparation of PtTPBP&BDPPA-Containing Polyurethane Film. The preparation of PtTPBP&BDPPA-containing polyurethane film followed a reported method with few modifications.^{17c,d} First, 2 g of polyurethane (10% in DMF) was mixed with 10 μL of PtTPBP (1.0×10^{-5} M) and 1 mL of BDPPA (1.5×10^{-3} M). The mixture solution was spin-coated onto a glass microscope slide, placed in an argon-saturated oven at 90 °C for 5 min, and then cooled to room temperature. Finally, the film was dried under vacuum for 24 h to completely remove the solvent.

Preparation of Assembly Film Composed of PtTPBP&BDPPA-Containing Polyurethane Film and Azotolane-Containing CLCP Film. The azotolane-containing CLCP film was prepared by thermal copolymerization of the mixture of LC monomer **1** and LC cross-linker **2** (Scheme 1b) with a molar ratio of 4:6 containing 4 mol % of a thermal initiator (2,2'-azobis(*N*-cyclohexyl-2-methylpropionamide). The mixture and the initiator were injected into a glass cell at 115 °C (a nematic phase), and the glass substrates were coated with polyimide alignment layers that had been rubbed to align the LC mesogens. The thermal polymerization was carried out in a vacuum oven under nitrogen at 115 °C for 24 h. The free-standing monodomain CLCP film was obtained by opening the cell and separating the film from the glass substrates. In addition, polydomain azotolane CLCP films were also prepared with the same process by injecting the polymerizable mixture into the glass cell whose polyimide layers had not been rubbed.

The assembly film was prepared by combining the azotolane-containing CLCP film and the PtTPBP&BDPPA-containing polyurethane film with a transparent adhesive or by directly spin-coating the DMF solution of polyurethane containing PtTPBP&BDPPA on the surface of the CLCP film.

Characterization. UV–vis absorption spectra were measured with a UV–vis absorption spectrophotometer (HITACH, U-4100). The UCL emission spectra were recorded with a fluorescence spectrophotometer (Edinburgh, FLS-920) using an external 0–500 mW adjustable 635 nm semiconductor laser (Changchun fs-optics Co., China) as the excitation source, instead of the xenon source in the spectrophotometer. The photos of UCL emission were obtained digitally on a multiple CCD camera (Panasonic, DMC-LX5GK). The thermal effect of CW 635 nm laser on the CLCP film was recorded by a thermal imaging camera (FLIR, E40). The glass transition temperature of polyurethane was determined by dynamic mechanical analysis (DMA; TA, Q800). Samples were prepared by cutting rectangular pieces from compression molded films of polyurethane. Measurements were taken at a frequency of 1 Hz with heating and cooling rates of 3 °C/min. Thermodynamic properties of the LC compounds **1** and **2** and the CLCP film were determined by differential scanning calorimetry (DSC; TA, Q2000) at heating and cooling rates of 3 °C/min for the LC compounds and 10 °C/min for the CLCP film, respectively. Three scans were applied to check the reproducibility. Visible light at 470 nm was obtained from an LED irradiator (CCS, PJ-1505-2CA). The optical anisotropy of the azotolane CLCP film was studied using a polarizing optical microscope (POM; Leica, DM2500p). The thickness of the films, photographs, and movie of the bending of the films as well as their bending angle

Scheme 1^a



^a(a) Illustration of TTA-UCL emission of the system composed of PtTPBP (sensitizer) and BDPPA (annihilator) under 635 nm excitation. The chemical structures of PtTPBP and BDPPA are also shown. (b) Chemical structures and properties of LC monomer **1** and cross-linker **2** used in this study. K, crystal; N, nematic; I, isotropic.

excitation at 635 nm, the PtTPBP&BDPPA system displayed an intense upconversion emission with a large anti-Stokes shift of 165 nm and a high absolute UCL quantum yield ($Q_{\text{Y,UCL}}$) of $9.3 \pm 0.5\%$. Furthermore, when PtTPBP&BDPPA was incorporated into a soft polyurethane film and then assembled with an azotolane-containing CLCP film, a new upconversion photoactuated soft material system with low-power, long-wavelength excitation was achieved. Importantly, we also demonstrated the advantages of using this novel red-light-controllable soft actuator in potential biological applications,

and time were taken by a super-resolution digital microscope (Keyence, VHX-1000C). The data of the time taken by the assembly film to bend by 30° upon CW 635 nm laser irradiation are the average value of measured data of three samples for three times in a certain power density. Detailed measurements of the absolute and relevant UCL efficiencies are described in the Supporting Information.

RESULTS AND DISCUSSION

UCL Property of PtTPBP&BDPPA in Toluene Solution.

It is well-known that 9,10-diphenylanthracene (DPA) is the famous annihilator exhibiting the highest upconversion efficiency of >20% (measured based on equation S2 in Supporting Information with an additional multiplicative factor of 2).^{17g,i} As a derivative of DPA, the compound BDPPA (Scheme 1a) also shows high fluorescence quantum yield of 95% (measured in toluene solution). Moreover, the replacement of diphenyl with bisphenylphosphoryl oxide at the 9,10-position causes a significant red shift in the emission band of BDPPA. The maximal fluorescence wavelengths of BDPPA are located at 470 and 485 nm, which are weakly overlapped between the Soret band and Q-band of the sensitizer PtTPBP, as shown in Figure S1. Therefore, it is expected that BDPPA is an ideal annihilator of the PtTPBP sensitizer.

Furthermore, the UCL property of PtTPBP&BDPPA in deaerated toluene was investigated before the preparation of the upconversion polymer film. Under excitation at 635 nm, PtTPBP&BDPPA displays intense blue UCL emission peaked at 470 and 485 nm, and the UCL intensity is enhanced as the incident laser power increases (Figure 1a). Moreover, the UCL

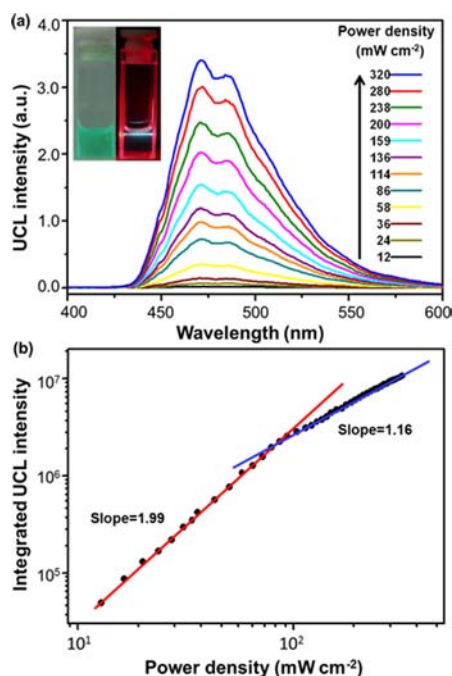


Figure 1. (a) UCL spectra of PtTPBP&BDPPA ($[PtTPBP] = 1.0 \times 10^{-5}$ M and $[BDPPA] = 1.5 \times 10^{-3}$ M) upon excitation of a CW 635 nm laser with different incident power densities. Inset: Photos of bright-field and photoluminescence emission (without any filter) of PtTPBP&BDPPA inside the 1 cm cuvette ($\lambda_{ex} = 635$ nm). UCL spectra of the toluene solution of PtTPBP&BDPPA at different concentration ratios of PtTPBP to BDPPA are shown in Figure S2 of Supporting Information. (b) Integrated UCL intensity data from part (a) plotted as a function of incident power density. All spectra are measured in deaerated toluene.

intensity shows quadratic dependence on the incident power in a lower power density region and linear dependence in a higher power density region. In the log–log plot, two linear fittings have been achieved with the slopes of 1.99 and 1.16 (Figure 1b). Such a relationship between the UCL emission intensity and the excitation power density confirms the photochemical nature of the TTA process.^{17j,20a,b} The qualitative Jablonski diagram of the TTA process is illustrated in Scheme S3. The absolute QY_{UCL} in deaerated toluene was measured to be $9.3 \pm 0.5\%$, which is the highest value reported for red-to-blue upconversion materials so far.^{21b,24} Moreover, the anti-Stokes shift is as high as 165 nm. PtTPBP&BDPPA also displayed high photostability as well as chemical stability, as shown in Figure S4 and Figure S5. Therefore, this excellent red-to-blue upconversion system PtTPBP&BDPPA is expected to be used as an ideal candidate for a highly effective phototrigger to induce the deformation of the azotolane CLCP film.

Photoisomerization of the Azotolane Moieties Induced by TTA-UCL.

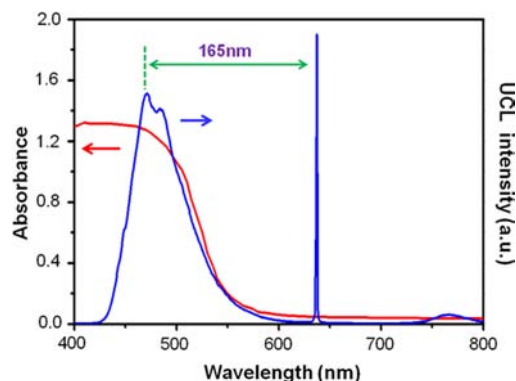


Figure 2. UCL emission spectrum (blue line) of the toluene solution of PtTPBP&BDPPA ($\lambda_{ex} = 635$ nm, power density = 200 mW cm^{-2}) and the UV–vis absorption spectrum (red line) of the azotolane CLCP film.

containing CLCP film exhibits a broad and strong absorption band between 400 and 500 nm, which matches well with upconversion emission peaks of PtTPBP&BDPPA in toluene, suggesting the rationale behind our choice of the azotolane-containing CLCP and the TTA-UCL system of PtTPBP&BDPPA. Therefore, it is assumed that the blue upconversion emission from PtTPBP&BDPPA could be absorbed by the azotolane moieties and subsequently trigger their *trans–cis* photoisomerization.

Moreover, two experiments were carried out to verify our hypothesis and provide the spectroscopic proof for the subsequent design of the soft actuators. In both of the experiments, the PtTPBP&BDPPA system and LC monomer **1** were filled in two separated quartz cells that were placed in close proximity. Figure 3a illustrates the layout of an experimental setup for the upconversion emission measurement. Interestingly, as Figure 3b shows, the intensity of transmitted UCL emission that peaked at 470 nm gradually decreases with the increase of the concentration of LC monomer **1** in cell 2, which is attributed to the reabsorption of the UCL emission by monomer **1**. This result indicates that the UCL emission can be effectively absorbed by the azotolane compounds through the emission–reabsorption process.

Furthermore, we also explored whether the *trans–cis* photoisomerization of the azotolane moieties can be triggered

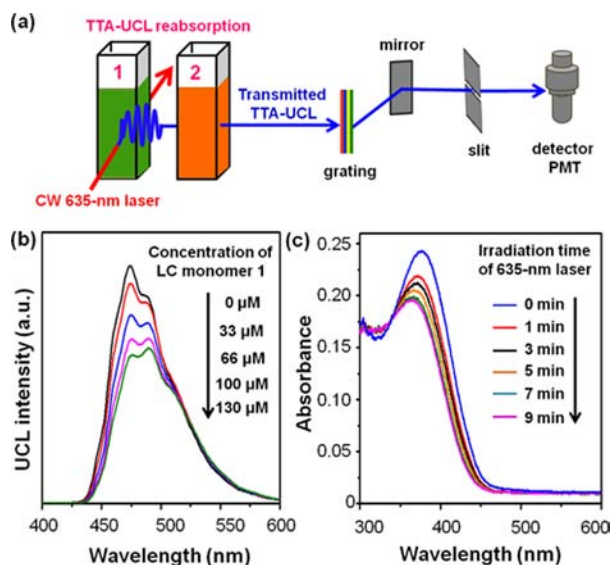


Figure 3. (a) Schematic layout of the UCL emission measurement system. CW 635 nm laser-irradiated PtTPBP&BDPPA in cell 1 to trigger TTA-UCL, and the generated blue emission went through cell 2 which was filled with the toluene solution of LC monomer 1. The transmitted TTA-UCL emission then passed through the grating instrument system and finally entered the photomultiplier tube (PMT) detector. The excitation laser beam path and the UCL emission pathway are shown in red and blue, respectively. (b) Change in the UCL intensity of transmitted TTA-UCL upon addition of different concentrations of toluene solution of LC monomer 1 in cell 2 under excitation at 635 nm (power density = 200 mW cm⁻²). (c) Change in the absorption spectra of the toluene solution of azotolane-containing LC monomer 1 (9.0×10^{-6} M) in cell 4 upon irradiation of blue TTA-UCL generated from excitation with a CW 635 nm laser in cell 3 (power density = 200 mW cm⁻²) for different times. (The layout of this UV-vis absorption measurement system is shown in Figure S6.)

by the blue UCL emission of PtTPBP&BDPPA via the emission–reabsorption process by using the experimental setup which is analogous to that in Figure 3a (Figure S6). The PtTPBP&BDPPA solution in cell 3 was first excited with the 635 nm laser to generate TTA-UCL emission, which was employed to irradiate the toluene solution of LC monomer 1 in cell 4. Importantly, after being irradiated with different time, the absorbance of a maximal absorption band at 385 nm of LC monomer 1 obviously decreased, corresponding to the *trans–cis* photoisomerization of the azotolane moieties (Figure 3c). However, in contrast, the direct irradiation of LC monomer 1 with the 635 nm laser induced very weak *trans–cis* photoisomerization of the azotolane moieties (Figure S7). These results confirm that the red-to-blue TTA-UCL emission of PtTPBP&BDPPA actually causes the *trans–cis* photoisomerization of the azotolane moieties in LC monomer 1.

UCL Property of PtTPBP&BDPPA in Solid-State Films.

In previous studies, the majority of efficient TTA-based upconversion systems have been carried out in liquid systems. However, to fully harness the potential of sensitized low-power upconversion in practical applications, it is highly desirable that an appropriate sensitizer/annihilator are embedded in solid materials for potential solid device integration^{17c,d,i} because their processability and mechanical characteristics are more suitable for many practical applications than liquid solutions.

In the present study, to achieve the integration of this TTA-based upconversion system with the CLCP, first, the

PtTPBP&BDPPA was incorporated into polyurethane with low glass transition temperature (Figure S8) because the rubbery polymers have been proven to be a very efficient solid platform to implement TTA-UCL,²⁵ due to the high translational molecular mobility of the chromophore molecules.^{17d,i,22c,25} Under selective excitation with a 635 nm laser, the PtTPBP&BDPPA-containing polyurethane film generated the intense blue UCL emission (see Figure 4a inset and Figure

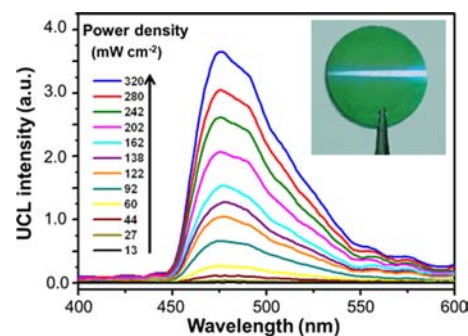


Figure 4. UCL spectra of the upconverting polyurethane film (containing 4 wt % PtTPBP&BDPPA, molar ratio of PtTPBP and BDPPA = 1:150) upon excitation of a CW 635 nm laser with different incident power densities. Inset: Emission photograph of upconverting polyurethane film with short-pass filter (edge wavelength at 628 nm). UCL spectra of the polyurethane films containing different concentrations of PtTPBP&BDPPA are shown in Figure S9 of Supporting Information.

S10 of Supporting Information) with absolute QY_{UCL} of $3.2 \pm 0.3\%$, indicating that the excellent UCL performance is still retained in the solid polyurethane matrix. Figure 4 also clearly demonstrates that the UCL intensity of the polyurethane film concomitantly increases with increasing incident power. Moreover, consistent with the solution state, the dependence of the UCL intensity on the incident power density exhibits the trend from quadratic to linear, giving two slopes of 2.05 and 1.20, respectively (Figure S11). Moreover, the upconverting polyurethane film showed excellent UCL stability upon exposure to the CW 635 nm laser for 1 h (Figure S12), demonstrating potential applications of this upconverting polyurethane film in practical photonic devices.

Photoinduced Bending Behavior of Assembly Film.

Before the preparation of the assembly film, the azotolane-containing CLCP film used in this work was synthesized by thermal copolymerization of the mixture of azotolane-containing LC monomer 1 and non-azotolane-containing LC cross-linker 2 (Scheme 1b), which is different from previously reported visible-light-driven CLCP films prepared from azotolane-containing monomer and cross-linker.^{6a,c} There are two advantages on this adjustment of the cross-linker: (1) the synthesis route of cross-linker 2 is less tedious than that of the previously used azotolane-containing cross-linker^{6a,c} (Scheme S2b); (2) the thermal polymerization is easier to achieve with the addition of cross-linker 2. As shown in Figure S13a, the mesogens in this prepared azotolane-containing CLCP film showed anisotropic alignment parallel to the rubbing direction, and it exhibited a glass transition temperature around 20 °C and a stable LC phase even when the temperature was higher than 180 °C (Figure S13b).^{6c}

The assembly film was prepared by combining the PtTPBP&BDPPA-containing polyurethane film and the azotolane CLCP film with transparent adhesive (Figure 5a).

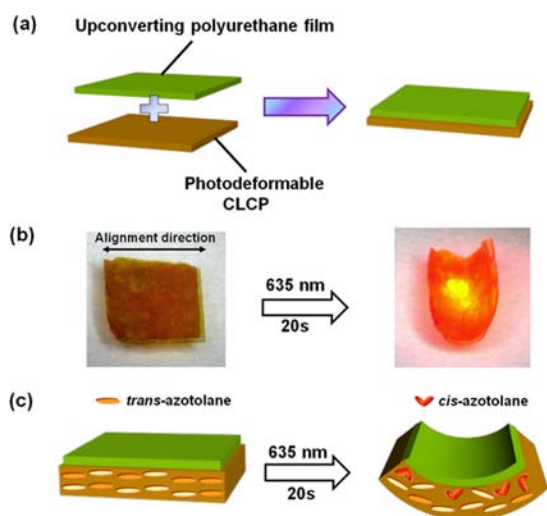


Figure 5. (a) Schematic illustration of the preparation of the assembly film composed of azotolane CLCP film and PtTPBP&BDPPA-containing polyurethane film. (b) Photographs of the as-prepared assembly film bending toward the light source along the alignment direction of the mesogens in response to the 635 nm laser with the power density of 200 mW cm^{-2} (thickness of each layer in the assembly film: $15 \mu\text{m}$ of upconverting film and $27 \mu\text{m}$ of CLCP). (c) Schematic illustration demonstrating plausible mechanism for the photoinduced deformation of the as-prepared assembly film.

As shown in Figure 5b, upon irradiation of the CW 635 nm laser with the power density as low as 200 mW cm^{-2} , the assembly film bent toward the light source along the alignment direction of the mesogens within 20 s.

Figure 5c illustrates our assumed mechanism for the photoinduced deformation of the assembly film: first, the PtTPBP&BDPPA-containing polyurethane film acts as an antenna to trap the 635 nm light and upconvert it into the blue TTA-UCL emission; then the TTA-UCL is absorbed by the azotolane moieties in the CLCP film via the emission–reabsorption process, which induces the *trans*–*cis* photoisomerization of the azotolane moieties and the subsequent alignment change of the mesogens. Due to the strong absorption of blue light of the azotolane moieties, the *trans*–*cis* photoisomerization and the alignment change of LC mesogens only occur in the front surface region of the azotolane CLCP film, which then leads to a contraction in this surface region, thus contributing to the photoinduced bending of the azotolane CLCP film toward the light source (Figure 5c).^{5–8,15}

After switching off the laser, the bent state was still retained, and the bent film reverted to the initial flat state within 60 s when heated to $80 \text{ }^\circ\text{C}$ (Figure S14), resulting from the *cis*–*trans* back thermal isomerization of the azotolane chromophores.²⁶

To simplify the preparation process, another bilayer film was also fabricated by spin-coating the DMF solution of polyurethane containing PtTPBP&BDPPA on the surface of the CLCP film. Importantly, this as-prepared assembly film also exhibited similar photoinduced bending behavior under exposure to the CW 635 nm laser, demonstrating the processing flexibility of the photodeformable CLCP assembly materials.

A set of control experiments were further designed to test the rationality of our assumed mechanism. Importantly, the

bending of a blank azotolane-containing CLCP film was triggered when irradiated directly with the TTA-UCL generated from a nearby, noncontacting PtTPBP&BDPPA-containing polyurethane film (Figure 6a), which indicates that

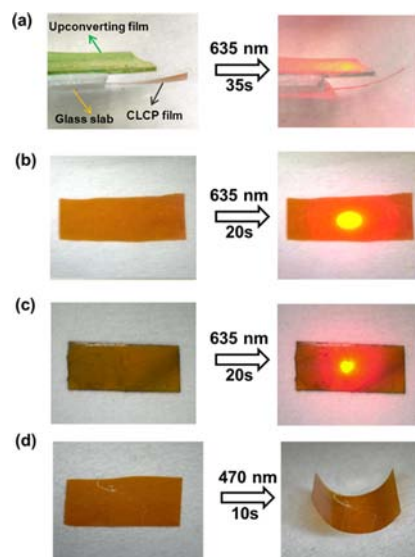


Figure 6. (a,b) Photographs of the blank azotolane CLCP film without upconverting polyurethane film containing PtTPBP&BDPPA upon irradiation of (a) the TTA-UCL generated from a nearby, noncontacting PtTPBP&BDPPA-containing polyurethane film (The CLCP film and the upconversion film are separated by a glass slab with the thickness of $150 \mu\text{m}$, and the thickness of the CLCP film and the upconversion film is 27 and $100 \mu\text{m}$, respectively) and (b) 635 nm light (200 mW cm^{-2}). (c) Photograph of the composite film composed of the CLCP film and the TTA-UCL chromophore powder without polyurethane upon irradiation of a 635 nm light with a power density of 200 mW cm^{-2} . (d) Photographs of the blank azotolane CLCP film upon irradiation of a 470 nm light (25 mW cm^{-2}). Thickness of the CLCP film is $27 \mu\text{m}$.

the thermal effect of the 635 nm light is not an issue here. When the blank azotolane-containing CLCP film without PtTPBP&BDPPA-containing polyurethane film was irradiated with a CW 635 nm laser, the CLCP film remained in the flat state (Figure 6b).

Furthermore, an assembly film composed of the CLCP film and the PtTPBP&BDPPA powder without polyurethane exhibited no bending behavior upon irradiation of the CW 635 nm laser either because the TTA-UCL emission is hardly generated from the mixed PtTPBP&BDPPA powder (Figure 6c). However, in contrast, the CLCP film exhibited bending behavior upon direct blue light irradiation at 470 nm, as a result of the *trans*–*cis* photoisomerization of the azotolane moieties and the alignment change of the mesogens in the surface region of the CLCP film (Figure 6d).^{6a,c} These control experiments imply that the introduction of the PtTPBP&BDPPA-containing polyurethane film is required to achieve the red-light-induced bending of the assembly film, for it is able to effectively utilize the 635 nm light and produce the red-to-blue TTA-UCL emission which subsequently triggers the bending of the CLCP film. (In addition, the movies showing the bending of the assembly film and unbending of the blank CLCP film upon irradiation of the CW 635 nm laser are available in Supporting Information.)

Moreover, experimental data of the anisotropic effect of azotolane mesogens on the deformation of the assembly film were obtained. When irradiated with the CW 635 nm laser, the square-shaped monodomain assembly film bent toward the light source along the rubbing direction of the polyimide alignment layers, whereas the bending direction of the square-shaped polydomain assembly film is random, due to its inhomogeneous alignment of the mesogens at the macroscopic scale (Figure S15). These results indicate that the bending deformation is ascribed to the *trans*–*cis* photoisomerization of the azotolane units and the following photochemically induced alignment change of the mesogens in the CLCP film driven by the blue TTA-UCL from the PtTPBP&BDPPA-containing polyurethane film. As far as we know, it is the first example achieving the assembly of upconverting rubbery films based on the TTA process into a photoresponsive solid device, in which the TTA-UCL is trapped and utilized to create a photo-mechanical effect.

The bending speed of the assembly film was measured upon irradiation of the CW 635 nm laser with different power intensities. Herein, the irradiation time taken by the film to bend by 30° was chosen as reference data. When the power density of the 635 nm laser was increased, the bending time decreased significantly (Figure S16). It is noted that the assembly film can still bend even with a low power density of 75 mW cm⁻² at 635 nm. This indicates that the new assembly film prepared in this work is able to be actuated by the 635 nm laser within a range of low power densities, illustrating great improvement compared with our previously reported NIR-light-responsive CLCP composite system driven by a high-power 980 nm laser (15 W cm⁻²).¹⁵

Moreover, the thermal effect induced by 635 nm irradiation with low power densities was also determined. As shown in Figure 7, after 635 nm irradiation with a power density of 200 mW cm⁻², the maximum temperature of the assembly film reached 23.0 °C with an increase of 3.1 °C. It is noteworthy that the temperature was kept at around 23.0 °C even when the

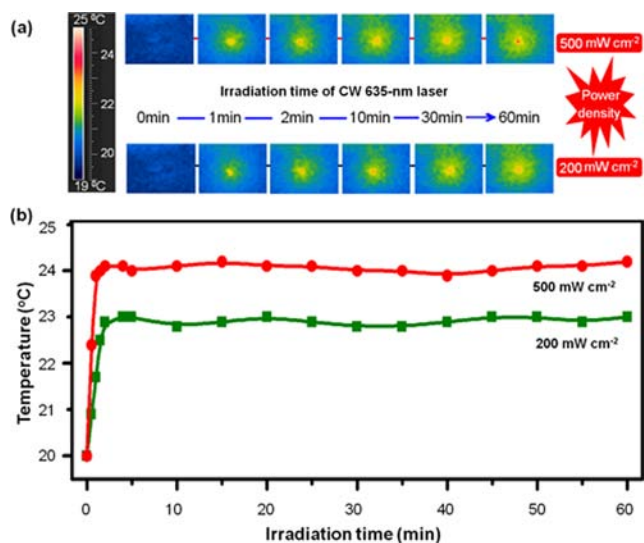


Figure 7. (a) Thermal photographs and (b) temperature changes from part (a) of the assembly film upon exposure to a CW 635 nm laser with two different power densities as a function of irradiation time (thickness of each layer in the assembly film: 15 μm of upconverting film and 27 μm of CLCP).

irradiation time was prolonged to 60 min. In addition, when the 635 nm laser with a higher power density of 500 mW cm⁻² was used to irradiate the assembly film for 60 min, the maximum temperature only reached 24.2 °C. Therefore, the thermal effect caused by the 635 nm laser is minimal, which is distinct from the overheating effect in our previous CLCP composite system with lanthanide upconversion nanoparticles ($\lambda_{\text{ex}} = 980 \text{ nm}$).¹⁵

From the viewpoint of negligible thermal effect of the low-power 635 nm laser on the CLCP film, this photodeformable assembly system would serve as promising photomechanical materials in potential bioapplications.²⁷ For the purpose of simple biological mimicking, a piece of pork with a thickness of 3 mm was put between the light source and the assembly film (Figure 8a). When the incident light at 635 nm (power density

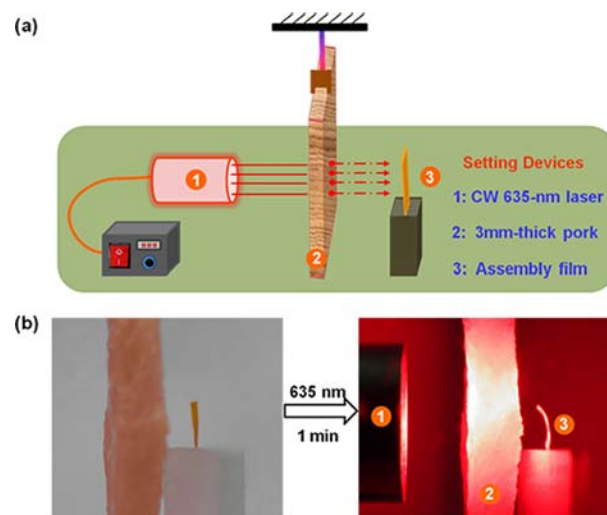


Figure 8. (a) Schematic illustration of the setup layout of investigating the photoinduced bending behavior of assembly film upon irradiation with a CW 635 nm laser (power density = 500 mW cm⁻²) when pork with thickness of 3 mm was put between the light source and the assembly film. (b) Photographs of assembly film bending toward the light source in response to the incident light transmitting through the pork (thickness of each layer in the assembly film: 15 μm of upconverting film and 27 μm of CLCP).

= 500 mW cm⁻²) was transmitted through the pork, the power density was reduced to 86 mW cm⁻²; however, the assembly film still bent toward the light source within 1 min (Figure 8b). This demonstrates the possibility of using 635 nm red light as an excitation source to induce the photodeformation of the CLCPs in biological systems because it can penetrate deeper in tissues and cause less harm to cells.²⁸

CONCLUSION

In this work, the strategy of utilizing the TTA-UCL technology as the low-power excited, long-wavelength phototrigger of the light-sensitive CLCP has been demonstrated. Initially, we achieved a highly effective red-to-blue TTA-based upconversion system with low-energy excitation light source, large anti-Stokes shift of 165 nm, and a high absolute quantum yield of $9.3 \pm 0.5\%$. To employ it as the phototrigger of the azotolane CLCP, this TTA-UCL system was incorporated into a rubbery polyurethane film and then assembled with azotolane-containing CLCP film. The resulting assembly film was able to be actuated by a 635 nm laser at a low power density due to the *trans*–*cis* photoisomerization of the azotolane moieties and

the alignment change of the mesogens induced by low-power excited blue TTA-UCL via an emission–reabsorption process. Moreover, the advantages of using this assembly film in potential biological applications have also been investigated as negligible thermal effect of a 635 nm laser and its excellent penetration ability into tissues.

In summary, we demonstrated the first example of the deformation of the CLCP triggered by red light at 635 nm, a wavelength that is orders of magnitude more penetrating through tissue than other parts of the short-wavelength visible spectrum and is less detrimental to biological tissues. Importantly, this work not only is a significant step forward to develop a novel red-light-controllable soft actuator based on TTA-UCL but also represents a new strategy on the technological applications of TTA-UCL in solid photonic devices.

■ ASSOCIATED CONTENT

■ Supporting Information

Preparation and characterization of TTA chromophores, upconverting film, CLCP films, and assembly film are included in the Supporting Information. The movies showing the bending of the assembly film and unbending of the blank CLCP film upon irradiation with a CW 635 nm laser are also included. This material is available free of charge via the Internet at <http://pubs.acs.org>.

■ AUTHOR INFORMATION

Corresponding Author

fyli@fudan.edu.cn; ylyu@fudan.edu.cn

Author Contributions

[§]Z.J. and M.X. contributed equally to this work.

Notes

The authors declare no competing financial interest.

■ ACKNOWLEDGMENTS

This research was supported by National Natural Science Foundation (51225304, 21273048, 21134003, and 21231004), National Research Fund for Fundamental Key Projects (2009CB930400), Shanghai Sci. Tech. Comm. (11QH1400400 and 12JC1401300). The authors thank Dr. Z. Shen and Y.C. Yang for kindly providing the BDPPA sample, and appreciate Dr. J.Z. Zhao for calculating the energy level of ³BDPPA*.

■ REFERENCES

- (1) (a) Yu, Y. L.; Ikeda, T. *Angew. Chem., Int. Ed.* **2006**, *45*, 5416–5418. (b) Wei, J.; Yu, Y. L. *Soft Matter* **2012**, *8*, 8050–8059. (c) Lendlein, A.; Jiang, H.; Junger, O.; Langer, R. *Nature* **2005**, *434*, 879–882.
- (2) (a) Ikeda, T.; Mamiya, J.; Yu, Y. L. *Angew. Chem., Int. Ed.* **2007**, *46*, 506–528. (b) Ohm, C.; Brehmer, M.; Zentel, R. *Adv. Mater.* **2010**, *22*, 3366–3387. (c) Yang, H.; Ye, G.; Wang, X. G.; Keller, P. *Soft Matter* **2011**, *7*, 815–823.
- (3) *Smart Light-Responsive Materials: Azobenzene-Containing Polymers and Liquid Crystal*; Zhao, Y., Ikeda, T. John Wiley & Sons, Inc.: Hoboken, NJ, 2009.
- (4) (a) Finkelmann, H.; Nishikawa, E.; Pereira, G. G.; Warner, M. *Phys. Rev. Lett.* **2001**, *8701*, 015501. (b) Cviklinski, J.; Tajbakhsh, A. R.; Terentjev, E. M. *Eur. Phys. J. E: Soft Matter Biol. Phys.* **2002**, *9*, 427–434. (c) Hogan, P. M.; Tajbakhsh, A. R. *Phys. Rev. E* **2002**, *65*, 041720. (d) Li, M.-H.; Keller, P.; Li, B.; Wang, X. G. *Adv. Mater.* **2003**, *15*, 569–572.

- (5) (a) Yu, Y. L.; Nakano, M.; Ikeda, T. *Nature* **2003**, *425*, 145. (b) Yu, Y. L.; Maeda, T.; Mamiya, J.; Ikeda, T. *Angew. Chem., Int. Ed.* **2007**, *46*, 881–883. (c) Yoshino, T.; Kondo, M.; Mamiya, J.; Kinoshita, M.; Yu, Y. L.; Ikeda, T. *Adv. Mater.* **2010**, *22*, 1361–1363.
- (6) (a) Cheng, F. T.; Yin, R. Y.; Zhang, Y. Y.; Yen, C.-C.; Yu, Y. L. *Soft Matter* **2010**, *6*, 3447–3449. (b) Wang, W.; Sun, X. M.; Wu, W.; Peng, H. S.; Yu, Y. L. *Angew. Chem., Int. Ed.* **2012**, *51*, 4644–4647. (c) Cheng, F. T.; Zhang, Y. Y.; Yin, R. Y.; Yu, Y. L. *J. Mater. Chem.* **2010**, *20*, 4888–4896.
- (7) Yamada, M.; Kondo, M.; Mamiya, J.; Yu, Y. L.; Kinoshita, M.; Barrett, C. J.; Ikeda, T. *Angew. Chem., Int. Ed.* **2008**, *47*, 4986–4988.
- (8) Yamada, M.; Kondo, M.; Miyasato, R.; Nakano, Y.; Mamiya, J.; Kinoshita, M.; Shishido, A.; Yu, Y. L.; Barrett, C. J.; Ikeda, T. *J. Mater. Chem.* **2009**, *19*, 60–62.
- (9) (a) White, T. J.; Tabiryan, N. V.; Serak, S. V.; Hrozhyk, U. A.; Tondiglia, V. P.; Koerner, H.; Vaia, R. A.; Bunning, T. J. *Soft Matter* **2008**, *4*, 1796–1798. (b) Serak, S.; Tabiryan, N.; Vergara, R.; White, T. J.; Vaia, R. A.; Bunning, T. J. *Soft Matter* **2010**, *6*, 779–783. (c) Lee, K. M.; Smith, M. L.; Koerner, H.; Tabiryan, N.; Vaia, R. A.; Bunning, T. J.; White, T. J. *Adv. Funct. Mater.* **2011**, *21*, 2913–2918.
- (10) van Oosten, C. L.; Bastiaansen, C. W. M.; Broer, D. J. *Nat. Mater.* **2009**, *8*, 677–682.
- (11) (a) Koerner, H.; Price, G.; Pearce, N. A.; Alexander, M.; Vaia, R. A. *Nat. Mater.* **2004**, *3*, 115–120. (b) Yang, L.; Setyowati, K.; Li, A.; Gong, S.; Chen, J. *Adv. Mater.* **2008**, *20*, 2271–2275. (c) Marshall, J. E.; Ji, Y.; Torras, N.; Kirill, Z.; Terentjev, E. M. *Soft Matter* **2012**, *8*, 1570–1574. (d) Moua, M.; Kohlmeyer, R. R.; Chen, J. *Angew. Chem., Int. Ed.* **2013**, *52*, 9234–9237. (e) de Haan, L. T.; Sánchez-Somolinos, C.; Bastiaansen, C. M. W.; Schenning, A. P. H. J.; Broer, D. J. *Angew. Chem., Int. Ed.* **2012**, *51*, 12469–12472.
- (12) (a) Auzel, F. *Chem. Rev.* **2004**, *104*, 139–173. (b) Haase, M.; Schäfer, H. *Angew. Chem., Int. Ed.* **2011**, *50*, 5808–5829.
- (13) Rachford, T. N. S.; Castellano, F. N. *Coord. Chem. Rev.* **2010**, *254*, 2560–2573.
- (14) (a) Carling, C. J.; Nourmohammadian, F.; Boyer, J. C.; Branda, N. R. *Angew. Chem., Int. Ed.* **2010**, *49*, 3782–3785. (b) Carling, C. J.; Boyer, J. C.; Branda, N. R. *J. Am. Chem. Soc.* **2009**, *131*, 10838–10839. (c) Yan, B.; Boyer, J.-C.; Branda, N. R.; Zhao, Y. *J. Am. Chem. Soc.* **2011**, *133*, 19714–19717. (d) Yan, B.; Boyer, J.-C.; Habault, D.; Branda, N. R.; Zhao, Y. *J. Am. Chem. Soc.* **2012**, *134*, 16558–16561.
- (15) Wu, W.; Yao, L. M.; Yang, T. S.; Yin, R. Y.; Li, F. Y.; Yu, Y. L. *J. Am. Chem. Soc.* **2011**, *133*, 15810–15813.
- (16) Parker, C. A.; Hatchard, C. G.; Joyce, T. A. *Nature* **1965**, *20*, 1282–1284.
- (17) (a) Singh-Rachford, T. N.; Haefele, A.; Ziesel, R.; Castellano, F. N. *J. Am. Chem. Soc.* **2008**, *130*, 16164–16165. (b) Islangulov, R. R.; Castellano, F. N. *Angew. Chem., Int. Ed.* **2006**, *45*, 5957–5959. (c) Islangulov, R. R.; Lott, J.; Weder, C.; Castellano, F. N. *J. Am. Chem. Soc.* **2007**, *129*, 12652–12653. (d) Singh-Rachford, T. N.; Lott, J.; Weder, C.; Castellano, F. N. *J. Am. Chem. Soc.* **2009**, *131*, 12007–12014. (e) Singh-Rachford, T. N.; Castellano, F. N. *J. Phys. Chem. A* **2008**, *112*, 3550–3556. (f) Khnayzer, R. S.; Blumhoff, J.; Harrington, J. A.; Haefele, A.; Deng, F.; Castellano, F. N. *Chem. Commun.* **2012**, *48*, 209–211. (g) Kim, J.-H.; Kim, J.-H. *J. Am. Chem. Soc.* **2012**, *134*, 17478–17481. (h) Cates, E. L.; Chinnapongse, S. L.; Kim, J.-H.; Kim, J.-H. *Environ. Sci. Technol.* **2012**, *46*, 12316–12328. (i) Kim, J.-H.; Deng, F.; Castellano, F. N.; Kim, J.-H. *Chem. Mater.* **2012**, *24*, 2250–2252. (j) Haefele, A.; Blumhoff, J.; Khnayzer, R. S.; Castellano, F. N. *J. Phys. Chem. Lett.* **2012**, *3*, 299–303.
- (18) (a) Liu, Q.; Yang, T.; Feng, W.; Li, F. Y. *J. Am. Chem. Soc.* **2012**, *134*, 5390–5397. (b) Liu, Q.; Yin, B.; Yang, T.; Yang, Y.; Shen, Z.; Yao, P.; Li, F. Y. *J. Am. Chem. Soc.* **2013**, *135*, 5029–5037.
- (19) (a) Ji, S. M.; Wu, W. H.; Wu, W. T.; Zhao, J. Z. *Angew. Chem., Int. Ed.* **2011**, *50*, 8283–8286. (b) Zhao, J. Z.; Wu, W. H.; Sun, J. F.; Guo, S. *Chem. Soc. Rev.* **2013**, *42*, 5323–5351. (c) Zhang, C. S.; Zhao, J. Z.; Wu, S.; Wang, Z. L.; Wu, W. H.; Ma, J.; Guo, S.; Huang, L. *J. Am. Chem. Soc.* **2013**, *135*, 10566–10578.
- (20) (a) Cheng, Y. Y.; Khoury, T.; Clady, R. G. C. R.; Tayebjee, M. J. Y.; Ekins-Daukes, N. J.; Crossley, M. J.; Schmidt, T. W. *Phys. Chem.*

Chem. Phys. **2010**, *12*, 66–71. (b) Monguzzi, A.; Mezyk, J.; Scotognella, F.; Tubino, R.; Meinardi, F. *Phys. Rev. B* **2008**, *78*, 195112. (c) Du, P. W.; Eisenberg, R. *Chem. Sci.* **2010**, *1*, 502–506. (d) Yamada, H.; Kuzuhara, D.; Ohkubo, K.; Takahashi, T.; Okujima, T.; Uno, H.; Ono, N.; Fukuzumi, S. *J. Mater. Chem.* **2010**, *20*, 3011–3024.

(21) (a) Balushev, S.; Miteva, T.; Yakutkin, V.; Nelles, G.; Yasuda, A.; Wegner, G. *Phys. Rev. Lett.* **2006**, *97*, 143903. (b) Balushev, S.; Yakutkin, V.; Miteva, T.; Wegner, G.; Roberts, T.; Nelles, G.; Yasuda, A.; Chernov, S.; Aleshchenkov, S.; Cheprakov, A. *New J. Phys.* **2008**, *10*, 013007. (c) Kastler, M.; Pisula, W.; Laquai, F.; Kumar, A.; Davies, R. J.; Balushev, S.; Garcia-Gutierrez, M. C.; Wasserfallen, D.; Butt, H. J.; Riekel, C.; Wegner, G.; Mullen, K. *Adv. Mater.* **2006**, *18*, 2255–2259. (d) Balushev, S.; Yakutkin, V.; Miteva, T.; Avlasevich, Y.; Chernov, S.; Aleshchenkov, S.; Nelles, G.; Cheprakov, A.; Yasuda, A.; Mullen, K.; Wegner, G. *Angew. Chem., Int. Ed.* **2007**, *46*, 7693–7696.

(22) (a) Monguzzi, A.; Frigoli, M.; Larpent, C.; Tubino, R.; Meinardi, F. *Adv. Funct. Mater.* **2012**, *22*, 139–143. (b) Monguzzi, A.; Tubino, R.; Hoseinkhani, S.; Campione, M.; Meinardi, F. *Phys. Chem. Chem. Phys.* **2012**, *14*, 4322–4332. (c) Monguzzi, A.; Bianchi, F.; Bianchi, A.; Mauri, M.; Simonutti, R.; Ruffo, R.; Tubino, R.; Meinardi, F. *Adv. Energy Mater.* **2013**, *3*, 680–686. (d) Monguzzi, A.; Tubino, R.; Meinardi, F. *J. Phys. Chem. A* **2009**, *113*, 1171–1174.

(23) (a) Yip, J. H. K.; Prabhavathy, J. *Angew. Chem., Int. Ed.* **2001**, *40*, 2159–2162. (b) Fei, Z. F.; Kocher, N.; Mohrschladt, C. J.; Ihmels, H.; Stalke, D. *Angew. Chem., Int. Ed.* **2003**, *42*, 783–787.

(24) (a) Singh-Rachford, T. N.; Castellano, F. N. *Inorg. Chem.* **2009**, *48*, 2541–2548. (b) Singh-Rachford, T. N.; Castellano, F. N. *J. Phys. Chem. Lett.* **2010**, *1*, 195–200. (c) Cheng, Y. Y.; Fückel, B.; MacQueen, R. W.; Khoury, T.; Clady, R.; Schulze, T. F.; Ekins-Daukes, N. J.; Crossley, M. J.; Stannowski, B.; Lips, K.; Schmidt, T. W. *Energy Environ. Sci.* **2012**, *5*, 6953–6959. (d) Murakami, Y.; Kikuchi, H.; Kawai, A. *J. Phys. Chem. B* **2013**, *117*, 2487–2494. (e) Turshatov, A.; Busko, D.; Balushev, S.; Miteva, T.; Landfester, K. *New J. Phys.* **2011**, *13*, 083035. (f) Cheng, Y. Y.; Fückel, B.; Khoury, T.; Clady, R. G.; Ekins-Daukes, N. J.; Crossley, M. J.; Schmidt, T. W. *J. Phys. Chem. A* **2011**, *115*, 1047–1053.

(25) Simon, Y. C.; Weder, C. *J. Mater. Chem.* **2012**, *22*, 20817–20830.

(26) Okano, K.; Shishido, A.; Ikeda, T. *Macromolecules* **2006**, *39*, 145–152.

(27) Woltman, S. J.; Jay, G. D.; Crawford, G. P. *Nat. Mater.* **2007**, *6*, 929–938.

(28) Samanta, S.; Beharry, A. A.; Sadowski, O.; McCormick, T. M.; Babalhavaeji, A.; Tropepe, V.; Woolley, G. A. *J. Am. Chem. Soc.* **2013**, *135*, 9777–9784.